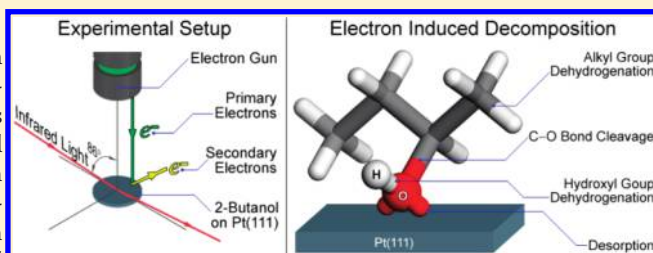


Thermal and Electron-Induced Decomposition of 2-Butanol on Pt(111)

Xiaofeng Hu,[†] Richard A. Rosenberg,[‡] and Michael Trenary^{*,†}[†]Department of Chemistry, University of Illinois at Chicago, Chicago, Illinois 60607, United States[‡]Advanced Photon Source, Argonne National Laboratory, Argonne, Illinois 60439, United States

ABSTRACT: The adsorption, thermal evolution, and electron irradiation of 2-butanol on Pt(111) were investigated with reflection absorption infrared spectroscopy (RAIRS). A simulated vibrational spectrum of a single 2-butanol molecule was calculated using density functional theory to facilitate vibrational assignments. Exposures of 0.2 Langmuir (L) and lower result in both isolated 2-butanol molecules with minimal lateral interactions and hydrogen-bonded clusters. The thermal evolution following a 4.0 L exposure shows that the hydrogen-bonded multilayer desorbs around 170 K, leaving a 2-butanol monolayer where hydrogen bonding still exists. At 190 K, a new feature at 1699 cm^{-1} is attributed to the formation of butanone. Irradiation with 750 or 100 eV electrons leads to 2-butanol desorption and partial conversion to butanone, as indicated by the appearance of a peak at 1709 cm^{-1} .



INTRODUCTION

Electron-induced reactions are of great interest in many different areas of science and technology from industrial plasmas to living tissues.^{1,2} The initial steps of electron-induced molecular decomposition include electron impact ionization, electron impact excitation, and electron attachment to form a transient negative ion.¹ In particular, the inelastic collisions of low-energy electrons with molecules and atoms produce distinct energetic species that are the primary driving forces in a wide variety of radiation-induced chemical reactions.² Examples include radiation damage in the DNA of living systems, electron-induced fragmentation of ozone, electron impact of etchant gases that react directly with the substrate in semiconductor processing, and electron-controlled chemistry using scanning tunneling microscopy.^{1,2} A very recent study demonstrated that low-energy, spin-polarized secondary electrons produced by X-ray irradiation of a magnetized Permalloy substrate can induce chiral-selective chemistry, an observation of relevance to theories on the creation of “handedness” in biological molecules.³ A 10% chiral enhancement on the cleavage rate of the C–O bond in a model chiral compound, (*R*)- or (*S*)-2-butanol, was observed to depend on the spin polarization of the X-ray-induced, low-energy secondary electrons and was attributed to dissociative electron attachment.³

The surface chemistry of saturated alcohols on transition metal surfaces has been reviewed by Mavrikakis and Barteau.⁴ The initial adsorption of alcohols generally occurs via donation of an oxygen lone pair of electrons to the surface. Cleavage of the O–H bond of alcohols upon their adsorption on transition metals leads to the formation of alkoxide intermediates, such as 2-butoxide/Pd(111),⁵ 2-propoxide/Ni(100),⁶ and 2-butoxide on Pt(111),⁷ which can further undergo β -hydride elimination to form a ketone. In a study of 2-butanol on Pt(111) by reflection absorption infrared spectroscopy (RAIRS),⁷ peaks at 1088 and

1112 cm^{-1} were assigned to $\nu(\text{CO})$ in monolayer and multilayer 2-butanol, respectively. The frequency shift of the CO stretching mode from 1112 to 1088 cm^{-1} is attributed to monolayer adsorption via the hydroxyl group. The absence of the in-plane O–H deformation, $\delta_{\text{ip}}(\text{OH})$, and CH deformation, $\delta(\text{CH})$, at 1158 and 1331 cm^{-1} , respectively, was attributed to the corresponding bonds being parallel to the surface. Between 170 and 200 K, the formation of surface 2-butoxide was inferred from the red shift of the asymmetric C–H stretches from those observed in 2-butanol and the red shift of the CO stretch from 1088 to 1084 cm^{-1} . In addition, the CH stretch bands are blue-shifted as the exposure increases.

In this work, electron irradiation of 2-butanol on Pt(111) was investigated with RAIRS. To have a thorough understanding of the electron-induced chemistry, the adsorption and thermal evolution of 2-butanol on Pt(111) were also reexamined. With the aid of vibrational frequencies calculated with density functional theory, we propose a few assignments that differ from those of Lee and Zaera,⁷ including the CO stretch and OH bending modes. A new feature at 1699 cm^{-1} , which is in a spectral region not shown in the work of Lee and Zaera,⁷ is observed during thermal evolution and assigned to the CO stretch of butanone. Secondary electrons can induce complex chemistry within the hydrogen-bonded 2-butanol multilayer, including multilayer desorption, dehydrogenation of the hydroxyl and alkyl groups, and C–O bond cleavage. Butanone, characterized by the CO stretch at 1709 cm^{-1} , is formed through

Special Issue: Victoria Buch Memorial

Received: September 9, 2010

Revised: November 30, 2010

Published: January 24, 2011

Table 1. Vibrational Frequencies for 2-Butanol: from a Simulation of the Tt Conformer of the Isolated Molecule,¹³ Following a 0.2 L Exposure at 95 K (monolayer), Following a 4.0 L Exposure at 95 K (multilayer), and after a 170 K Anneal Following a 4.0 L Exposure at 95 K

	simulated spectrum	monolayer	multilayer	postannealed monolayer
$\nu(\text{OH})$	3499	3100–3500	3130–3380	3100–3500
$\nu_{\text{a}}(\text{CH}_3)$	2984		2966	
$\nu_{\text{a}}(\text{CH}_2)$	2961	2956	2939	2955, 2949
$\nu_{\text{s}}(\text{CH}_3)$	2899	2939	2931	2929
$\nu_{\text{s}}(\text{CH}_2)$	2869	2914	2910	2908
$\nu(\text{CH})$	2936		2881	2887, 2883
$\delta_{\text{a}}(\text{CH}_3)$	1492	1460	1485, 1468, 1460	1466, 1458
$\gamma(\text{CH}_2), \delta_{\text{a}}(\text{CH}_3)$	1477	1448, 1443	1446, 1427	1446
$\delta_{\text{s}}(\text{CH}_3)$	1392	1404	1416	1398
$\delta(\text{CH}), \delta_{\text{ip}}(\text{OH})$	1361	1377	1375	1375
wag(CH_2), $\delta(\text{CH})$	1348		1362	1360
$\delta(\text{CH}), \text{twist}(\text{CH}_2)$	1300		1337, 1302	1313
$\delta_{\text{ip}}(\text{OH}), \rho(\text{CH}_3)$	1231		1255	1250, 1273
$\nu(\text{CO}), \rho(\text{CH}_3)$	1151	1151, 1117, 1084	1163, 1128, 1113	1153, 1113
$\nu(\text{CC}), \rho(\text{CH}_3)$	1101			
$\delta_{\text{ip}}(\text{OH}), \rho(\text{CH}_3)$	1053		1090	1090
$\nu(\text{CC}), \rho(\text{CH}_3)$	984	1029	1034	1028
$\rho(\text{CH}_3)$	961	987	993, 966	989, 964
$\nu(\text{CO}), \rho(\text{CH}_3)$	869	885	916	893

bonds in water or alcohol can enhance the OH stretch signal by 250%.¹⁴ The 2-butanol solution shows a peak at 3630 cm^{-1} , which is at essentially the same position relative to the strongly red-shifted hydrogen-bonded OH stretch as observed in a study of a series of liquid alcohols and alcohol solutions, for which it is assigned to a “free” (not hydrogen-bonded) OH stretch.¹⁵ The RAIR spectrum for 4.0 L of 2-butanol on Pt(111) is quite similar to the solution phase spectrum, including the broad and red-shifted hydrogen-bonded OH stretch. The comparison also implies that a 4.0 L exposure leads to a multilayer of 2-butanol with a condensed phase structure similar to that found in solution. However, unlike in the solution, a “free” OH stretch is not observed for multilayer 2-butanol.

Also shown in Figure 1 are spectra for monolayer 2-butanol prepared in two different ways. Spectrum d is for a 0.2 L exposure with the crystal at 95 K, whereas spectrum e is for a surface that had been annealed to 170 K following a 4.0 L exposure of 2-butanol at 95 K. Comparing spectra d and e suggests that if the “post-annealed” case represents approximately one monolayer, then the 0.2 L exposure gives a submonolayer coverage. However, even for a submonolayer coverage, a broad, red-shifted OH stretch is still visible, indicating that the molecules can hydrogen bond to each other even while they are in contact with the planar surface.

The inset in Figure 1 is an expanded view of the 2-butanol solution spectrum, which reveals a weak peak at 1728 cm^{-1} . This could be due either to a contaminant, likely a ketone, or to a combination band. Either explanation would also apply to the multilayer 2-butanol spectrum in which a peak is seen at 1699 cm^{-1} . Because this is also in the region of the intense C=O stretch of butanone, contamination of standard sources of 2-butanol with small amounts of butanone is a likely explanation. The vibrational simulation allows for further insights into some of the details of the spectra of 2-butanol on Pt(111). The simulation indicates that there are two normal modes with fundamentals at 869 and

1151 cm^{-1} that have large contributions from both the C–O stretch and the CH_3 rock. In the simulations in ref 13, three modes, calculated to be at 1110, 1124, and 1136 cm^{-1} , are described as being of mixed CO stretching and C*CH bending character, with C* being the carbon bonded to the oxygen atom. In a study of ethanol and deuterium-substituted analogues on preoxidized Cu(100), symmetric and asymmetric CCO stretches were assigned to peaks at 881 and 1091.¹⁶ The shift of $\nu_{\text{s}}(\text{CCO})$ from 1097 cm^{-1} in $\text{CH}_3\text{CH}_2\text{OH}$ to 1044 cm^{-1} in $\text{CD}_3\text{CH}_2\text{OH}$ is attributed to a reduced mixing of $\nu_{\text{s}}(\text{CCO})$ with $\rho(\text{CD}_3)$ compared with $\nu_{\text{s}}(\text{CCO})$ with $\rho(\text{CH}_3)$.¹⁶ The intensity patterns in Figure 1 for 0.2 and 4.0 L spectra suggest that the 916 cm^{-1} and 1113/1128 cm^{-1} peaks in the multilayer correlate with the 885 and 1084 cm^{-1} peaks, respectively, in the monolayer. This is consistent with the idea that the CO bond is weakened and, hence, modes with CO stretch character are red-shifted in the monolayer due to interaction of the CO bond with the surface. Thus, for 0.2 L of 2-butanol on Pt(111), the features at 885 and 1084 cm^{-1} as shown in Figure 1 are assigned to $\nu(\text{CO})/\rho(\text{CH}_3)$ in monolayer 2-butanol. The peak assignments are summarized in Table 1 and are generally in accord with previous studies.^{5,7,12,13,17–19}

Similarly, the simulation shows that two normal modes with fundamentals at 1053 and 1231 cm^{-1} have large contributions from the in-plane OH bend, $\delta_{\text{ip}}(\text{OH})$, and $\rho(\text{CH}_3)$. In 2-butanol solutions with concentrations below 0.1 M in which hydrogen bonding is minimal, $\delta_{\text{ip}}(\text{OH})$ contributes to two strong vibrational features at 1072 and 1242 cm^{-1} , but at higher concentrations, these features disappear as hydrogen bonding becomes more prevalent.^{12,13} The fact that peaks corresponding to the 1072 and 1242 cm^{-1} peaks are not prominent, if present at all, for the monolayer spectra in Figure 1, is consistent with the presence of hydrogen bonding. The absence of a peak near 1242 cm^{-1} in spectrum d also argues against associating the peak observed at 1084 cm^{-1} with the one seen by Shin et al.¹² at 1072 cm^{-1} and at

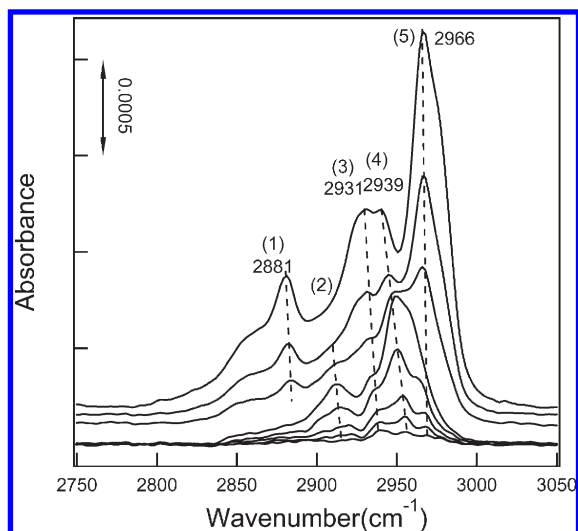


Figure 2. CH stretch region of 2-butanol on Pt(111). From top to bottom, the exposures were 4.0, 2.0, 1.5, 1.0, 0.5, 0.2, 0.1, and 0.05 L. Some spectra are offset for clarity. The peaks from 1 to 5 are assigned to $\nu(\text{CH})$, $\nu_s(\text{CH}_2)$, $\nu_s(\text{CH}_3)$, $\nu_a(\text{CH}_2)$, and $\nu_a(\text{CH}_3)$, respectively.

1076 cm^{-1} by Wang and Polavarapu,¹³ assigned to COH + CCH bending by the latter.

For the CH stretches in Figure 2, as the exposure increases, the peaks generally shift to the red, likely as a combined result of molecule–substrate interaction, molecular reorientation, and intermolecular interactions. The assignment follows the rule of thumb $\nu_s(\text{CH}_2) < \nu_s(\text{CH}_3) < \nu_a(\text{CH}_2) < \nu_a(\text{CH}_3)$.¹⁹ With respect to $\nu_a(\text{CH}_2)$, $\nu_a(\text{CH}_3)$ has a lower intensity below 1.0 L, has a comparable intensity between 1.0 and 1.5 L, and has a higher intensity above 1.5 L. The relative intensity change of $\nu_a(\text{CH}_3)$ and $\nu_a(\text{CH}_2)$ is attributed to the interaction between the CH_3 groups and the Pt surface for monolayer 2-butanol. Similar to $\nu_a(\text{CH}_3)$, the minimal intensity of $\nu(\text{CH})$ at low exposures is attributed to the interaction between the CH group and the Pt surface. At exposures higher than 1.0 L, $\nu(\text{CH})$ in multilayer 2-butanol contributes a feature at 2881 cm^{-1} .

Exposure Dependence of 2-Butanol Spectra. Figure 3 shows RAIR spectra as a function of 2-butanol exposure to Pt(111) at 90 K. At 0.05 L, only $\delta_a(\text{CH}_3)$ at $\sim 1450\text{ cm}^{-1}$ and the CH stretching bands between 2800 and 3000 cm^{-1} are detectable. At 0.1 L, peaks at 885 and 1151 cm^{-1} and a broad feature due to $\nu(\text{OH})$ at 3100 – 3500 cm^{-1} start to appear. As the exposure increases, self-association in 2-butanol clusters enhances hydrogen bonding, causing the broadening and red-shifting of the $\nu(\text{OH})$ band.¹⁵ At 0.2 L, several new features between 850 and 1450 cm^{-1} appear, including the peak at 1084 cm^{-1} assigned to $\nu(\text{CO})$, as noted in Table 1. At 0.5 L, the features at 885 and 1151 cm^{-1} start to show high-frequency shoulders, which are associated with $\nu(\text{CO})$ and $\rho(\text{CH}_3)$ in clustered 2-butanol. They develop into the features at 916 and 1163 cm^{-1} for the 4.0 L exposure and are assigned to $\nu(\text{CO})/\rho(\text{CH}_3)$ in multilayer 2-butanol. At 1.0 L, the features at 885 and 1084 cm^{-1} associated with $\nu(\text{CO})$ in monolayer 2-butanol reach maximum intensity, indicating completion of the monolayer for this exposure. The features at 1800 and 2089 cm^{-1} are attributed to CO molecules from the background that occupy hollow sites and atop sites, respectively.²⁰ As the exposure of 2-butanol increases, atop CO is displaced to hollow site CO, as indicated by the diminishing

intensity of the atop CO at 2089 cm^{-1} accompanied by increasing intensity of the hollow-site CO at 1800 cm^{-1} .

For monolayer adsorption, saturated alcohols adsorb on transition metal surfaces via the oxygen lone pair with additional weak van der Waals-type bonding between the alkyl group and the metal surface.^{4,21} In the right panel of Figure 3, an OH stretch at 3321 cm^{-1} appears to be superimposed on the broader OH stretch typical of hydrogen bonding, suggesting that at the lowest coverages, some 2-butanol molecules have a different bonding environment compared with the majority of the molecules. The 3321 cm^{-1} peak is both strongly red-shifted from where it would be for the isolated molecule, indicating a strong interaction via the oxygen lone pair with the metal surface, and relatively narrow, indicating minimal lateral interactions with other adsorbed 2-butanol molecules. This is similar to low coverages of D_2O on Pt(111), where a strong Pt–O interaction induces a large red shift of the OH stretch band.²² The differences in the CH stretching bands between 0.05 and 4.0 L are likely due to a combination of changes in adsorbate–substrate interactions, reorientation effects, and changes in adsorbate–adsorbate interactions.

Thermal Evolution of 2-Butanol. Figure 4 shows a series of RAIR spectra of 2-butanol/Pt(111) as a function of annealing temperature. The clean Pt(111) surface at 95 K was first dosed with 4.0 L of 2-butanol, and a RAIR spectrum was recorded. After a 30 s anneal at 160 K, another RAIR spectrum was collected once the sample had cooled back to 95 K. The above steps were repeated for several annealing temperatures until no discernible IR features were observed.

The intensity decrease of all the features between 95 and 170 K is attributed to multilayer desorption. The vibrational features around 916 and 1163 cm^{-1} persist to 170 K, indicating multilayer desorption around this temperature. The intensities of $\rho(\text{CH}_3)$ at 964 cm^{-1} and $\nu(\text{OH})$ at 3255 cm^{-1} are slightly enhanced at 170 K compared with those at 165 K, which is attributed to the formation of a crystalline phase of 2-butanol.²³ At 170 K, the features associated with the CH stretch modes have similar intensities compared with those for 1.0 L of 2-butanol, as shown in Figure 3, which indicates approximately the same coverage in the two cases. The OH stretch that remains visible up to 210 K is attributed to the hydrogen-bonded 2-butanol monolayer. Similar to water, a hydrogen bond in an alcohol forms when the hydrogen atom in a hydroxyl group interacts with a lone pair of electrons on the oxygen atom of another hydroxyl group. The hydrogen bonding in the 2-butanol monolayer suggests that only one of the two electron lone pairs on the oxygen atom interacts with the Pt surface, with the other lone pair available for hydrogen bonding.

It has been proposed that on transition metal surfaces, the hydroxyl group in saturated alcohols can be dehydrogenated to form alkoxide intermediates, such as 2-butoxide/Pd(111),⁵ 2-propoxide/Ni(100),⁶ and 2-butoxide on Pt(111),⁷ which can further undergo β -hydride elimination to form a ketone. Unlike methoxy and ethoxy that have strong CO stretches at 1008 and 1034 cm^{-1} , respectively, on preoxidized Cu(100),^{16,24} vibrational characteristics of 2-butoxide are not readily apparent here. In particular, for 2-butanol, there is no single normal mode that is dominated by the CO stretch, and the same is likely true for 2-butoxide. Rather, several modes have large contributions from both CO stretch and CCH bending coordinates. The red shift of a peak at 1088 – 1084 cm^{-1} reported by Lee and Zaera⁷ indicating a conversion of 2-butanol to 2-butoxide is not readily apparent in our spectra. Sexton, et al., reported that less than 10%

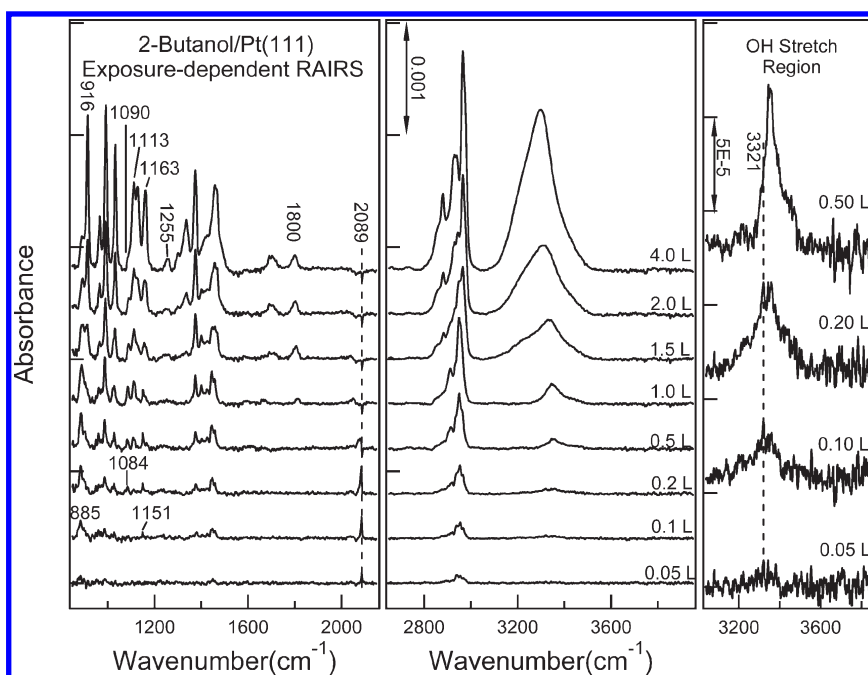


Figure 3. RAIR spectra of 2-butanol on Pt(111) as a function of exposure at 90 K. The spectra in the right panel were collected at 4 cm^{-1} resolution with an InSb detector, a tungsten source, and 1024 scans.

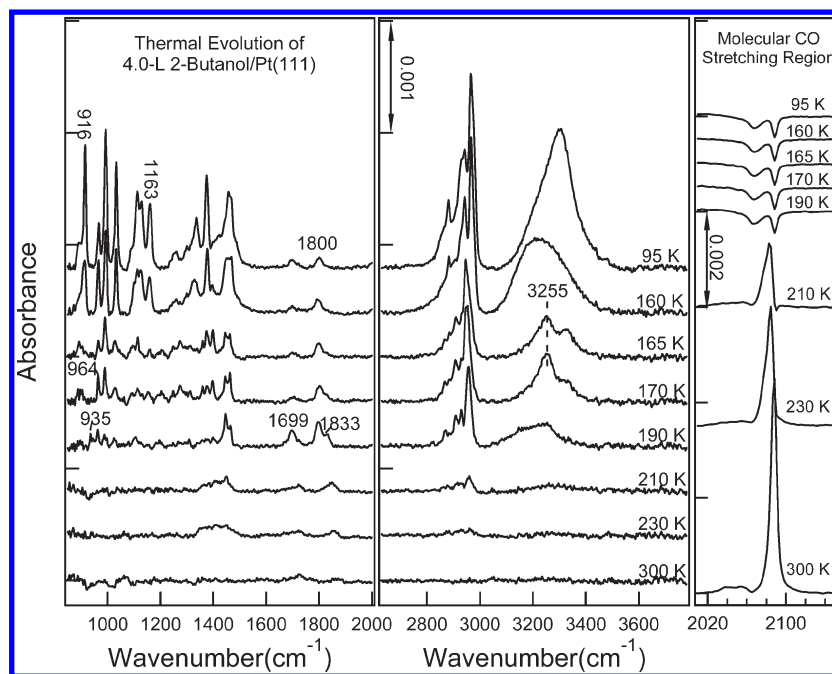


Figure 4. RAIR spectra of the thermal evolution of 2-butanol on Pt(111) in the temperature range of 90–300 K.

of an adsorbed monolayer dissociates, with 90% of the alcohol desorbing intact for C_1 – C_4 saturated alcohols on clean Pt(111).²⁵ The amount of 2-butoxide present on the surface is likely to be low, although it is the likely intermediate for the formation of the small amount of butanone, which we do observe.

C_1 – C_4 saturated alcohols on Pt(111) can decompose to CO, H, and C.²⁶ The spectra of Figure 4 reveal several changes with annealing temperature in peaks associated with adsorbed CO.

CO molecules at hollow sites, bridge sites, and atop sites have frequencies of ~ 1800 , 1833 , and 2089 cm^{-1} , respectively.²⁰ There is inevitably a small amount of background CO adsorbed on the Pt(111) surface, and the negative intensity features in the 2040 – 2010 cm^{-1} region, accompanied by the appearance of a positive peak at 1800 cm^{-1} , indicates that the adsorption of 2-butanol displaces CO from atop to hollow sites. These features associated with atop CO remain unchanged up to 190 K, whereas a shoulder at 1833 cm^{-1} begins to develop at 160 K and becomes

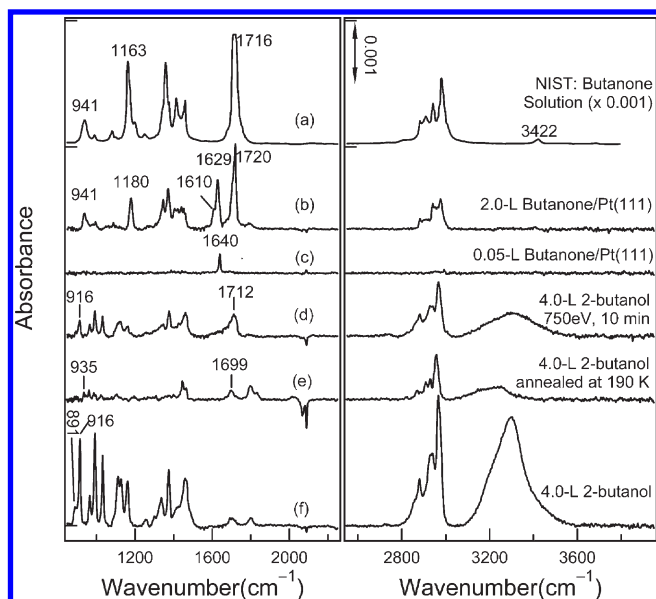


Figure 5. Infrared spectra of (a) butanone solution, (b) 2.0-L butanone/Pt(111), (c) 0.5-L butanone/Pt(111), (d) 4.0-L 2-butanol/Pt(111) after irradiation with 750-eV electrons for 10 min, (e) 4.0-L 2-butanol/Pt(111) annealed at 190 K, and (f) 4.0-L 2-butanol/Pt(111) prior to electron irradiation.

quite distinct by 190 K. With the 210 K anneal, there is a large increase in the atop CO, as indicated by the strong peak at 2080–2100 cm⁻¹, accompanied by a decrease in all other peaks. These changes indicate that the fraction of 2-butanol that does not desorb molecularly dissociates to form CO starting at temperatures between 190 and 210 K. It was already noted that the atop CO molecules due to background adsorption are displaced to hollow sites by the uptake of 2-butanol molecules.

To identify the formation of butanone from 2-butanol, five infrared spectra are plotted for comparison in Figure 5. The top spectrum is for butanone solution (10% in CCl₄ for 1300–3800 cm⁻¹ and 10% in CS₂ for 650–1300 cm⁻¹).¹⁰ The most intense peak at 1716 cm⁻¹ is assigned to the CO stretch, the overtone of which is at 3422 cm⁻¹. The next two RAIR spectra are of butanone on Pt(111) following exposures of 2.0 and 0.05 L. At 0.05 L, the CO stretch is at 1640 cm⁻¹ for monolayer butanone. At 2.0 L, the feature at 1720 cm⁻¹ is attributed to the CO stretch of multilayer butanone, and the CO stretch of monolayer butanone is red-shifted to 1629 cm⁻¹ with a shoulder at 1610 cm⁻¹. Both for the butanone solution and for 2.0 L of butanone on Pt(111), a feature due to $\rho(\text{CH}_3)$ of the CH₃ group is seen at 941 cm⁻¹.¹⁰ The second spectrum from the bottom is of 2-butanol/Pt(111) after annealing to 190 K. The new features at 935 and 1699 cm⁻¹ are assigned to $\rho(\text{CH}_3)$ of the CH₃ group and the CO stretch, respectively, of butanone in an η^1 -configuration where the molecule is bonded to the surface via the oxygen atom.^{4,27} Although a peak is observed at ~ 1700 cm⁻¹ in Figure 3 for the 2-butanol multilayer, its intensity relative to the other 2-butanol peaks is higher in Figure 5, supporting the idea that some of the 2-butanol thermally decomposes to form butanone on Pt(111). In contrast, on Pd(111), a much larger peak at 1670 cm⁻¹ due to butanone formation from 2-butanol thermal decomposition is observed.⁵ The presence of butanone is consistent with 2-butoxide formation via dehydrogenation of the hydroxyl group in 2-butanol, followed by β -hydride elimination

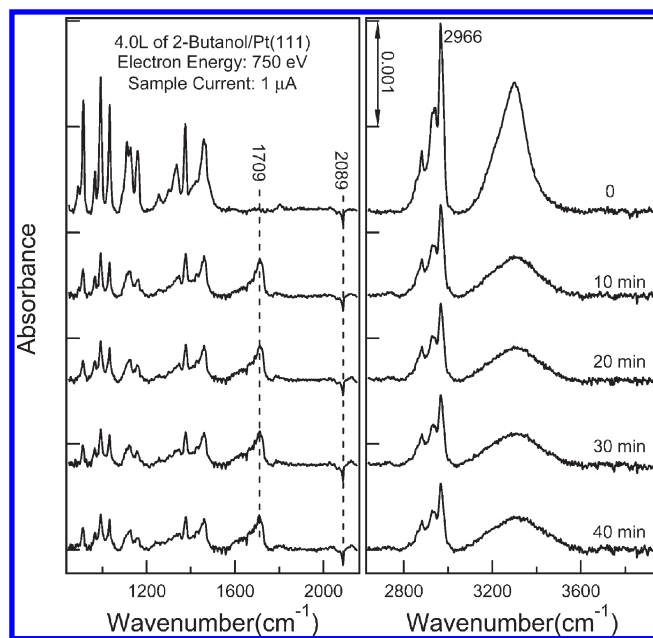


Figure 6. RAIR spectra of electron-induced decomposition of 4.0-L 2-butanol on Pt(111) as a function of time at an electron energy of 750 eV and a sample current of +1.0 μA .

to form butanone. However, unlike 2-butoxide, it is possible to detect a low coverage of butanone because of the very strong and well isolated C=O stretch of the carbonyl group.

Electron Induced Decomposition of 2-Butanol. Figure 6 shows RAIR spectra of 4.0 L of 2-butanol on Pt(111) at 90 K as a function of time under irradiation from the LEED gun with 750 eV electrons at an average sample current of +1.0 μA . Because the secondary emission yield and backscattered electron yield at 750 eV are 1.5 and 0.4, respectively,^{28,29} a positive sample current is consistent with the net loss of electrons. At 10 min, a new feature at 1709 cm⁻¹ appears, and the vibrational features associated with 2-butanol decrease significantly compared with those at time zero. As the comparison in Figure 5 indicates, this new feature is close to the value of 1720 cm⁻¹ for the C–O stretch for 2.0 L of butanone on Pt(111), which corresponds to a butanone multilayer. This suggests that the electron-induced formation of butanone occurs in the 2-butanol multilayer.

Figure 6 shows that the development of the peak at 1706 cm⁻¹ is accompanied by a uniform decrease of all peaks due to 2-butanol, with little change in the relative intensities of these peaks. After 10 min of irradiation, the intensity of the 916 cm⁻¹ peak, associated with multilayer 2-butanol, decreases by $\sim 75\%$, whereas the peak height of $\nu_2(\text{CH}_3)$, at 2966 cm⁻¹, decreases by more than 50% to reach a value similar to that of 1.5 L of 2-butanol in Figure 3. The similarity of the 2-butanol features between 0 and 10 min suggests that the remaining 2-butanol molecules have a structure similar to that in the multilayer phase, indicating that electron-stimulated desorption of the 2-butanol multilayer is partly responsible for the intensity drop. Electron-stimulated desorption was also observed for a methanol (CH₃OD) multilayer on Ti(001) at 80 K under the bombardment of electrons at an energy of 65 eV, where time-of-flight mass spectra show multiple desorption products, including H, CH, CH₂, and CH₃.³⁰

Figure 7 shows RAIR spectra versus irradiation time by 750 eV electrons at a sample current of +1.0 μA of a 2-butanol

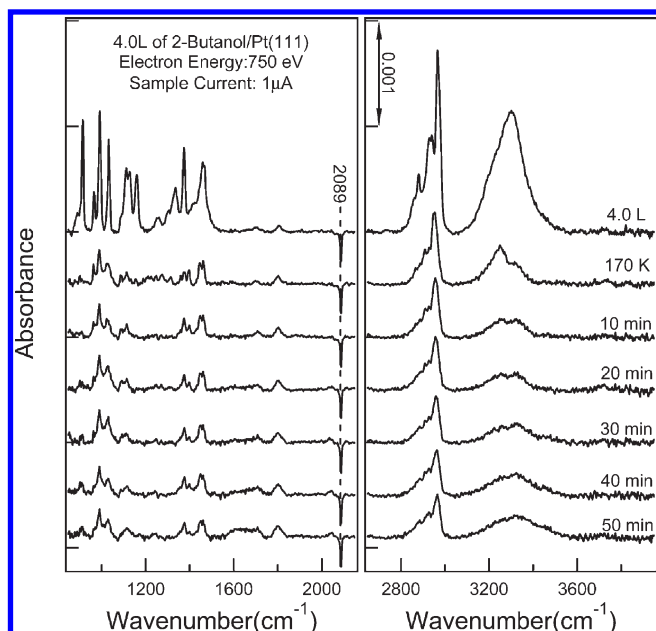


Figure 7. Time-dependent RAIR spectra of a 2-butanol monolayer on Pt(111) irradiated by 750 eV electrons at a sample current of $+1.0 \mu\text{A}$. The monolayer was prepared by first exposing 4.0 L of 2-butanol to the Pt(111) surface at 90 K, followed by annealing to 170 K to desorb the multilayer.

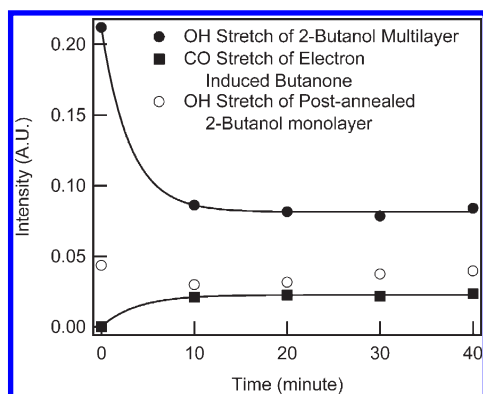


Figure 8. Time-dependent intensity of the OH stretch in multilayer 2-butanol, the CO stretch of the formed butanone in multilayer 2-butanol, and the OH stretch in a postannealed monolayer 2-butanol under the irradiation of electrons. The postannealed 2-butanol monolayer is obtained by annealing the 2-butanol multilayer at 170 K.

monolayer on Pt(111) obtained by annealing the multilayer to 170 K. The intensities of all features associated with the 2-butanol monolayer diminish over time, which is attributed to electron-induced decomposition. A broad feature develops between 1550 and 1750 cm^{-1} . This is likely due to the carbonyl group of a ketone species, similar to the case of the 2-butanol multilayer in which butanone is identified. There is a slight increase in CO occupation at hollow sites (around 1800 cm^{-1}) and atop sites (around 2050 cm^{-1}), which can be a result of electron-induced decomposition of 2-butanol. The OH stretch drops in height, but the width increases. Figure 8 shows a plot of the vibrational intensities versus electron irradiation time for the CO stretch of butanone and the OH stretch of multilayer 2-butanol based on the spectra of Figure 6, and the OH stretch of 2-butanol following

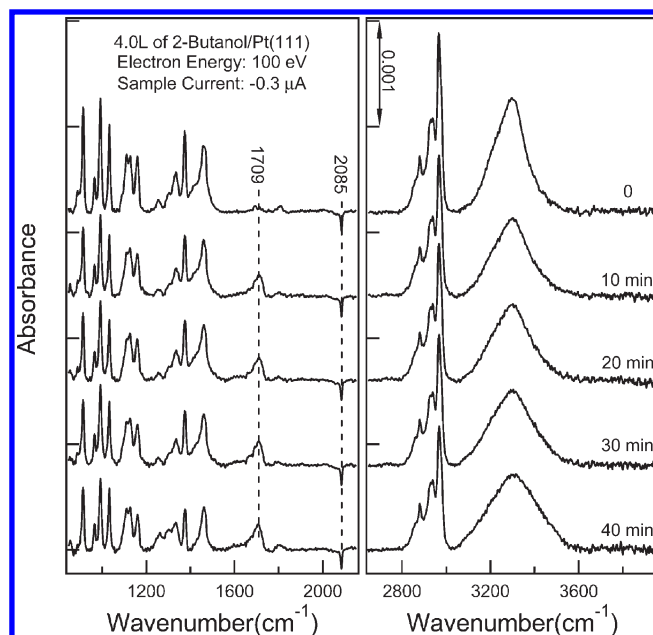


Figure 9. RAIR spectra of electron-induced decomposition of 4.0-L 2-butanol on Pt(111) as a function of time at an electron energy of 100 eV and a sample current of $-0.3 \mu\text{A}$.

annealing to 170 K to desorb the multilayer, based on the spectra of Figure 7. The lack of significant changes after 10 min of irradiation indicates that after multilayer desorption and reaction within the multilayer, the remaining adsorbates are largely unaffected by the electron beam.

In Figure 9, a similar experiment with 100 eV electrons and a sample current of $-0.3 \mu\text{A}$ shows a lower extent of decrease of the 2-butanol features and formation of butanone compared with the 750 eV case. To estimate the flux of secondary electrons, it is assumed that only primary, secondary, and backscattered electrons, noted as I_{PE} , I_{SE} , and I_{BE} , respectively, contribute to the sample current: $I_{\text{SE}} + I_{\text{BE}} - I_{\text{PE}} = I_{\text{sample}}$. I_{SE} and I_{BE} can be determined from $I_{\text{SE}} = \delta I_{\text{PE}}$ and $I_{\text{BE}} = \eta I_{\text{PE}}$, where δ and η are the secondary emission yield ($<50 \text{ eV}$) and backscattered electron yield ($>50 \text{ eV}$), respectively. The choice of 50 eV as the border between secondary and backscattered electrons is arbitrary.²⁸ Thus, we can obtain

$$I_{\text{PE}} = \frac{I_{\text{sample}}}{\delta + \eta - 1} \quad (1)$$

The parameters of the electron–surface interactions are summarized in Table 2. It can be seen that I_{PE} is very similar in both cases, where the beam energy and sample current are 750 eV and $+1 \mu\text{A}$, and 100 eV and $-0.3 \mu\text{A}$, respectively. I_{BE} at 750 eV is greater by a factor of 4 compared with that at 100 eV. This is consistent with the fact that a larger decrease in the infrared peaks occurs for 750 eV electrons than for 100 eV electrons.

The RAIRS results presented here for 2-butanol on Pt(111) can potentially offer additional insights into the XPS study of (R)- and (S)-2-butanol adsorbed on a magnetized $\text{Fe}_{0.2}\text{Ni}_{0.8}$ Permalloy substrate, where changes in the C 1s peak under the irradiation of X-rays was observed.³ In both cases, multilayers of 2-butanol were studied at a low temperature of 85–90 K. In the XPS study, low-energy, spin-polarized secondary electrons were assumed to induce decomposition via dissociative electron

Table 2. Electron–surface Interaction Parameters^a

energy (eV)	δ	η	I_{sample} (μA)	I_{PE} (μA)	I_{SE} (μA)	I_{BE} (μA)	f_{SE} (e/s)
750	1.5	0.4	1.0	1.1	1.7	0.4	1×10^{13}
100	0.7	0.05	-0.3	1.2	0.8	0.1	5×10^{12}

^a δ , secondary emission yield of platinum; η , backscattered electron yield of platinum; I_{PE} , current of primary electrons; I_{SE} , current of secondary electrons; I_{BE} , current of backscattered electrons; f_{SE} , flux of secondary electrons. δ and η at 750 eV are obtained from the literature, and δ and η at 100 eV are estimated values.^{28,29}

attachment. A chiral enhancement on the decomposition rate was observed, depending on the polarization of the secondary electrons. In comparing RAIRS and XPS results, it is important to recognize the differences in the type of information provided by the two techniques. In general, XPS has less chemical specificity than RAIRS but is more quantitative. Thus, whereas two separate C 1s components attributable to the one carbon atom in 2-butanol bound to oxygen (C–O) versus the three carbon atoms bound only to hydrogen (C–H) were identified, it is not clear that XPS would be able to detect a shift in the C–O binding energy for conversion of 2-butanol to butanone. While this reaction is readily apparent with RAIRS, owing to the strong IR intensity of the C=O stretch of butanone, it is difficult to estimate the fraction of the 2-butanol that converts to butanone from the RAIRS results. It may be such a small amount that even if the C 1s binding energies were measurably different, the reaction might not be detectable with XPS.

From the RAIRS data, it is clear that an overall decrease in the vibrational peak intensities under electron irradiation is largely due to electron-induced desorption. This is likely also a factor in the decreases in the C–H and C–O XPS peaks associated with 2-butanol, although this was not explicitly considered at that time.³ A subsequent reanalysis of the XPS data revealed decreases in overall peak areas consistent with some electron-induced desorption in addition to scission of the C–O bond to form other surface intermediates.³¹ This latter conclusion was supported by the observation of an increase in a C 1s XPS peak attributable to carbon bound directly to the metal substrate, C–M. Decomposition of 2-butanol involving C–O bond cleavage might not yield surface intermediates with detectable RAIRS peaks, and therefore, the lack of evidence here for C–O bond cleavage does not rule out such a reaction. Although these RAIRS experiments were intended to provide insights into electron-induced reactions of 2-butanol on a metal surface, the experimental conditions are quite different from those of Rosenberg, et al.³ In particular, because of the small area of the X-ray beam, the electron flux density was about an order of magnitude higher than used in our experiments. Thus, it would not be surprising for more complete degradation of the 2-butanol layer to occur in the XPS study. Our results suggest, however, that butanone is likely to have been an intermediate in the decomposition pathway in their experiment, as well.

CONCLUSIONS

The adsorption, thermal evolution, and electron-induced decomposition of 2-butanol on Pt(111) were investigated with reflection absorption infrared spectroscopy (RAIRS). 2-Butanol adsorbs molecularly on Pt(111) at 90 K. At exposures of 0.2 L and lower, it either adsorbs as an isolated species, indicated by a

sharp OH stretch at 3321 cm^{-1} , or forms hydrogen-bonded clusters. The thermal evolution of 4.0 L of 2-butanol between 95 and 300 K shows that the hydrogen-bonded multilayer desorbs around 170 K, revealing a monolayer where hydrogen bonding still exists. A crystalline phase of 2-butanol, indicated by enhanced intensities of $\rho(\text{CH}_3)$ at 964 cm^{-1} and $\nu(\text{OH})$ at 3255 cm^{-1} , is also observed at 170 K. The remaining hydrogen-bonded monolayer includes 2-butanol molecules and a small amount of surface 2-butoxide. At 190 K, the surface 2-butoxide undergoes β -hydride elimination to form butanone, which is characterized by a C–O stretch at 1699 cm^{-1} . Secondary electrons can induce complex chemistry within the hydrogen-bonded 2-butanol multilayer, including multilayer desorption, dehydrogenation of the hydroxyl and alkyl groups, and C–O bond cleavage. Butanone is formed through the electron-induced dehydrogenation of the hydroxyl and CH groups in 2-butanol and is characterized by a C–O stretch at 1709 cm^{-1} .

AUTHOR INFORMATION

Corresponding Author

*E-mail: mtrenary@uic.edu.

ACKNOWLEDGMENT

We thank Professor W. T. Tysoe of the University of Wisconsin–Milwaukee for helpful discussions. This work was supported by Argonne National Laboratory and by the National Science Foundation under Grant CHE-1012201.

REFERENCES

- (1) Arumainayagam, C. R.; Lee, H. L.; Nelson, R. B.; Haines, D. R.; Gunawardane, R. P. *Surf. Sci. Rep.* **2010**, *65*, 1.
- (2) Mason, N. J. *AIP Conf. Proc.* **2003**, *680*, 885.
- (3) Rosenberg, R. A.; Abu Haija, M.; Ryan, P. J. *Phys. Rev. Lett.* **2008**, *101*, 101.
- (4) Mavrikakis, M.; Barteau, M. A. *J. Mol. Catal. A: Chem.* **1998**, *131*, 135.
- (5) Stacchiola, D.; Burkholder, L.; Tysoe, W. T. *J. Am. Chem. Soc.* **2002**, *124*, 8984.
- (6) Gleason, N.; Guevremont, J.; Zaera, F. *J. Phys. Chem. B* **2003**, *107*, 11133.
- (7) Lee, I.; Zaera, F. *J. Phys. Chem. B* **2005**, *109*, 12920.
- (8) Brubaker, M. E.; Trenary, M. *J. Chem. Phys.* **1986**, *85*, 6100.
- (9) Malik, I. J.; Brubaker, M. E.; Mohsin, S. B.; Trenary, M. *J. Chem. Phys.* **1987**, *87*, 5554.
- (10) Coblenz Society, Inc. Evaluated Infrared Reference Spectra. In *NIST Chemistry WebBook, NIST Standard Reference Database Number 69*; Linstrom, P. J.; Mallard, W. G., Eds.; National Institute of Standards and Technology: Gaithersburg, MD 20899; <http://webbook.nist.gov>.
- (11) Frisch, M. J.; Trucks, G. W.; Schlegel, H. B.; Scuseria, G. E.; Robb, M. A.; Cheeseman, J. R.; Montgomery, J. A., Jr.; Vreven, T.; Kudin, K. N.; Burant, J. C.; Millam, J. M.; Iyengar, S. S.; Tomasi, J.; Barone, V.; Mennucci, B.; Cossi, M.; Scalmani, G.; Rega, N.; Petersson, G. A.; Nakatsuji, H.; Hada, M.; Ehara, M.; Toyota, K.; Fukuda, R.; Hasegawa, J.; Ishida, M.; Nakajima, T.; Honda, Y.; Kitao, O.; Nakai, H.; Klene, M.; Li, X.; Knox, J. E.; Hratchian, H. P.; Cross, J. B.; Bakken, V.; Adamo, C.; Jaramillo, J.; Gomperts, R.; Stratmann, R. E.; Yazyev, O.; Austin, A. J.; Cammi, R.; Pomelli, C.; Ochterski, J. W.; Ayala, P. Y.; Morokuma, K.; Voth, G. A.; Salvador, P.; Dannenberg, J. J.; Zakrzewski, V. G.; Dapprich, S.; Daniels, A. D.; Strain, M. C.; Farkas, O.; Malick, D. K.; Rabuck, A. D.; Raghavachari, K.; Foresman, J. B.; Ortiz, J. V.; Cui, Q.; Baboul, A. G.; Clifford, S.; Cioslowski, J.; Stefanov, B. B.; Liu, G.;

Liashenko, A.; Piskorz, P.; Komaromi, I.; Martin, R. L.; Fox, D. J.; Keith, T.; Al-Laham, M. A.; Peng, C. Y.; Nanayakkara, A.; Challacombe, M.; Gill, P. M. W.; Johnson, B.; Chen, W.; Wong, M. W.; Gonzalez, C.; Pople, J. A. *Gaussian 03*; Gaussian, Inc.: Wallingford, CT, 2003.

- (12) Shin, S.; Nakata, M.; Hamada, Y. *J. Phys. Chem. A* **2006**, *110*, 2122.
- (13) Wang, F.; Polavarapu, P. L. *J. Phys. Chem. A* **2000**, *104*, 10683.
- (14) Luck, W. A. P. *J. Mol. Struct.* **1998**, *448*, 131.
- (15) Palombo, F.; Paolantoni, M.; Sassi, P.; Morresi, A.; Cataliotti, R. S. *J. Mol. Liq.* **2006**, *125*, 139.
- (16) Camplin, J. P.; McCash, E. M. *Surf. Sci.* **1996**, *360*, 229.
- (17) Berman, N. S.; McKetta, J. J. *J. Phys. Chem.* **1962**, *66*, 1444.
- (18) Gao, P.; Lin, C. H.; Shannon, C.; Salaita, G. N.; White, J. H.; Chaffins, S. A.; Hubbard, A. T. *Langmuir* **1991**, *7*, 1515.
- (19) Socrates, G. *Infrared Characteristic Group Frequencies*, 2nd ed.; Wiley-Interscience: New York, 1994.
- (20) Hayden, B. E.; Bradshaw, A. M. *Surf. Sci.* **1983**, *125*, 787.
- (21) Rendulic, K. D.; Sexton, B. A. *J. Catal.* **1982**, *78*, 126.
- (22) Ogasawara, H.; Yoshinobu, J.; Kawai, M. *Chem. Phys. Lett.* **1994**, *231*, 188.
- (23) Lucas, S.; Ferry, D.; Demirdjian, B.; Suzanne, J. *J. Phys. Chem. B* **2005**, *109*, 18103.
- (24) Mudalige, K.; Trenary, M. *J. Phys. Chem. B* **2001**, *105*, 3823.
- (25) Sexton, B. A.; Rendulic, K. D.; Hughes, A. E. *Surf. Sci.* **1982**, *121*, 181.
- (26) Greeley, J.; Mavrikakis, M. *J. Am. Chem. Soc.* **2002**, *124*, 7193.
- (27) Anton, A. B.; Avery, N. R.; Toby, B. H.; Weinberg, W. H. *J. Am. Chem. Soc.* **1986**, *108*, 684.
- (28) Gomati, M. M. E.; Walker, C. G. H.; Assa'd, A. M. D.; Zdražil, M.; Zcaron, I. *Scanning* **2008**, *30*, 2.
- (29) Walker, C. G. H.; El-Gomati, M. M.; Assa'd, A. M. D.; Zdražil, M. *Scanning* **2008**, *30*, 365.
- (30) Stockbauer, R.; Bertel, E.; Madey, T. E. *J. Chem. Phys.* **1982**, *76*, 5639.
- (31) Rosenberg, R. A. Private communication.